

Emergence of pion parton distributions

Z.-F. Cui (崔著钊)^{1,2}, M. Ding (丁明慧)³, J. M. Morgado⁴, K. Raya^{5,6}, D. Binosi^{7,*}, L. Chang (常雷)^{8,†},
F. De Soto⁹, C. D. Roberts^{1,2,‡}, J. Rodríguez-Quintero^{4,§}, and S. M. Schmidt^{3,10,||}

¹*School of Physics, Nanjing University, Nanjing, Jiangsu 210093, China*

²*Institute for Nonperturbative Physics, Nanjing University, Nanjing, Jiangsu 210093, China*

³*Helmholtz-Zentrum Dresden-Rossendorf, Bautzner Landstraße 400, D-01328 Dresden, Germany*

⁴*Department of Integrated Sciences and Center for Advanced Studies in Physics,
Mathematics and Computation, University of Huelva, E-21071 Huelva, Spain*

⁵*Departamento de Física Teórica y del Cosmos, Universidad de Granada, E-18071 Granada, Spain*


⁶*Instituto de Ciencias Nucleares, Universidad Nacional Autónoma de México,
Apartado Postal 70-543, CDMX 04510, México*

⁷*European Centre for Theoretical Studies in Nuclear Physics and Related Areas,
Villa Tambosi, Strada delle Tabarelle 286, I-38123 Villazzano (TN), Italy*

⁸*School of Physics, Nankai University, Tianjin 300071, China*

⁹*Departamento Sistemas Físicos, Químicos y Naturales, Universidad Pablo de Olavide, E-41013 Sevilla, Spain*

¹⁰*RWTH Aachen University, III. Physikalisches Institut B, Aachen D-52074, Germany*

 (Received 3 January 2022; revised 7 March 2022; accepted 20 April 2022; published 20 May 2022)

Supposing only that there is an effective charge which defines an evolution scheme for parton distribution functions (DFs) that is all-orders exact, strict lower and upper bounds on all Mellin moments of the valence-quark DFs of pionlike systems are derived. Exploiting contemporary results from numerical simulations of lattice-regularized quantum chromodynamics (QCD) that are consistent with these bounds, parameter-free predictions for pion valence, glue, and sea DFs are obtained. The form of the valence-quark DF at large values of the light-front momentum fraction is consistent with predictions derived using the QCD-prescribed behavior of the pion wave function.

DOI: [10.1103/PhysRevD.105.L091502](https://doi.org/10.1103/PhysRevD.105.L091502)

I. ISSUES AND MOTIVATIONS

Within the Standard Model of particle physics, hadrons emerged roughly $1 \mu\text{s}$ after the big bang [1]. At this time, the color-carrying gluon and quark (parton) degrees-of-freedom, in terms of which the Lagrangian of quantum chromodynamics (QCD) is expressed, were sublimated into color-singlet bound states with nuclear-size masses and femtometre-scale radii. Pions (π^\pm , π^0) are the lightest hadrons; and without them, even simple nuclei could not have formed in the ensuing few minutes [2, Sec. 24]. Additionally, and crucially for the stability of nuclei, pions are unnaturally light: compared with the masses of the protons and neutrons (m_N) they bind, $m_\pi \approx 0.15m_N$.

This is explained if the pions are Nambu-Goldstone (NG) bosons associated with dynamical chiral symmetry breaking in QCD [3–5]. That raises some very basic questions, e.g.,: what imprints, if any, does this NG boson character leave on pion structure; and does it distinguish their structure and interactions from those of the nucleons they bind?

In QCD, pions are bound-states seeded by a valence-quark and valence-antiquark, Fig. 1. Yet, their properties cannot be determined by solving a typical two-body problem in quantum mechanics. Owing to strong self-interactions among gluons—QCD’s gauge bosons, the Lagrangian gluon and quark partons are transmogrified into complex quasiparticles. Each parton species evolves to acquire a distinct dynamically generated running mass [6–8], both of which are large at infrared momenta and typified by a renormalization group invariant mass $m_0 \approx m_N/2$; and the interactions between these quasiparticles are described by a momentum dependent coupling [9,10], $\hat{\alpha}(k^2)$, which runs to saturate at infrared momenta: $\hat{\alpha}(k^2 \lesssim m_0^2) \approx \pi$. These features are primary signals of the dynamical breaking of scale invariance in QCD [11], i.e., the phenomenon of emergent hadron mass (EHM). They produce a pion whose structure, when unfolded in terms of

*binosi@ectstar.eu

†leichang@nankai.edu.cn

‡cdroberts@nju.edu.cn

§jose.rodriguez@dfaie.uhu.es

||s.schmidt@hzdr.de

Published by the American Physical Society under the terms of the [Creative Commons Attribution 4.0 International license](https://creativecommons.org/licenses/by/4.0/). Further distribution of this work must maintain attribution to the author(s) and the published article’s title, journal citation, and DOI. Funded by SCOAP³.

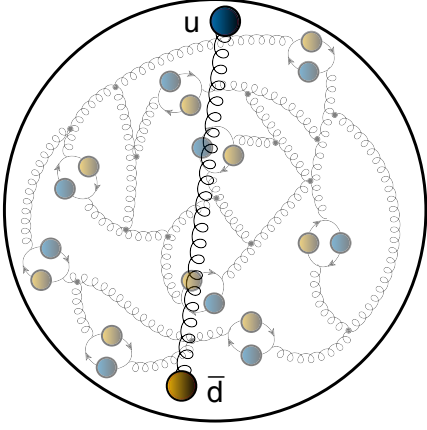


FIG. 1. In terms of QCD's Lagrangian degrees-of-freedom, the π^+ contains one valence u -quark, one valence \bar{d} -quark, and, owing to the strong-interaction, infinitely many gluons and sea quarks, indicated here as “springs” and closed loops, respectively. (π^- is $d\bar{u}$ and π^0 is $u\bar{u} - d\bar{d}$).

parton degrees-of-freedom, has the complicated character illustrated in Fig. 1, and may lead to gluon and quark confinement [12,13].

Continuum Schwinger function methods (CSMs) [14–17] are well suited to tackling the pion. Successes have been achieved by solving the coupled quark gap and meson Bethe-Salpeter equations to obtain the pion's Bethe-Salpeter wave function, $\chi_\pi(k, k - P)$, where P is the pion's total momentum and k is the momentum of the valence-quark, and exploiting that to predict pion observables [8,18]. Of great importance to an explanation of pion properties, is the expression of an intimate link between the dressed-quark mass function and χ_π [19–24]. This link means that, although it can be studied using a large array of reactions [17,25–27], the sharpest probes of EHM are found in pion properties; raising pion structure studies to the highest level of importance [28–34].

Much is promised by data relating to pion parton distribution functions (DFs), *viz.* the probability densities describing the light-front momentum fractions carried by each parton species within the pion [35]. For instance, $\mathbf{u}^\pi(x; \zeta)$ is the density for finding a valence u -quark with momentum fraction x when the pion is resolved at scale ζ . On $\zeta \lesssim 2m_N$, this valence-quark is not equivalent to a valence-quark-parton; rather, it is connected to that parton as an object dressed by interactions in the manner described by the quark gap equation [36]. Undressing reveals the complexities in Fig. 1, leading to growth of the glue and sea-quark DFs, $\mathbf{g}^\pi(x)$, $\mathcal{S}^\pi(x)$. However, more than forty years after the first experiment to collect data suitable for extracting pion DFs [37–40], the behavior of all these functions remains uncertain and controversial [41,42]: some analyses potentially challenge QCD as the theory of strong interactions. New experiments [28–34] will hopefully serve to dispel the confusion.

II. SYMMETRY AND PION WAVE FUNCTIONS

Notwithstanding the intricacies of Fig. 1, simplicity emerges when one adapts CSMs to the pion problem. Then, at infrared scales, the π^+ , for instance, appears as a two-body bound-state of a dressed-valence-quark, u , and a dressed-valence-antiquark \bar{d} , with the complexity hidden from view because the infinitely many gluon and quark partons have been absorbed into making the dressed quasiparticles. In this case, exploiting the \mathcal{G} -parity symmetry limit, which is an accurate reflection of Nature,

$$\chi_\pi(k, k - P) = \chi_\pi(-k + P, -k). \quad (1)$$

Unlike wave functions in quantum mechanics, χ_π does not have a probability interpretation; hence, cannot directly yield $\mathbf{u}^\pi(x; \zeta)$. That door is opened by projection to obtain the associated light-front wave function (LFWF) [43,44], $\psi_\pi(x, |\vec{k}_\perp|^2; \zeta)$, which is a probability amplitude. Here, using linearly independent four-vectors n , \bar{n} , with $n^2 = 0 = \bar{n}^2$, $n \cdot \bar{n} = -1$: $x = n \cdot k / n \cdot P$, *i.e.*, the light-front fraction of the pion's total momentum carried by the valence-quark; and \vec{k}_\perp is that part of the valence-quark's momentum which lies in the light-front transverse plane.

Using the LFWF,

$$\mathbf{u}^\pi(x; \zeta) \stackrel{x \in (0,1)}{=} H_\pi^u(x, t = 0; \zeta), \quad (2)$$

where H_π^u is the valence u -quark forward generalized parton distribution [45], and:

$$H_\pi^u(x, 0; \zeta) = \int \frac{d^2 k_\perp}{16\pi^3} |\psi_\pi^u(x, k_\perp^2; \zeta)|^2. \quad (3)$$

The LFWF defined by projection of $\chi_\pi(k, k - P)$ is associated with a scale, $\zeta = \zeta_{\mathcal{H}}$, at which the dressed-quark and -antiquark carry all pion properties and Eq. (1) entails $\psi_\pi^u(x, |\vec{k}_\perp|^2; \zeta_{\mathcal{H}}) = \psi_\pi^u(1 - x, |\vec{k}_\perp|^2; \zeta_{\mathcal{H}})$. Hence,

$$\mathbf{u}^\pi(x; \zeta_{\mathcal{H}}) = \mathbf{u}^\pi(1 - x; \zeta_{\mathcal{H}}), \quad (4)$$

$$\langle 2x \rangle_{\mathbf{u}^\pi}^{\zeta_{\mathcal{H}}} := \int_0^1 dx 2x \mathbf{u}^\pi(x; \zeta_{\mathcal{H}}) = 1, \quad (5)$$

confirming that dressed valence degrees-of-freedom carry all the pion's light-front momentum at this scale. Momentum conservation demands that the glue and sea momentum fractions vanish at $\zeta_{\mathcal{H}}$; and since DFs are nonnegative on $x \in [0, 1]$, then $\mathbf{g}^\pi(x; \zeta_{\mathcal{H}}) \equiv 0 \equiv \mathcal{S}^\pi(x; \zeta_{\mathcal{H}})$.

As the resolving scale is increased to $\zeta > \zeta_{\mathcal{H}}$, the dressed-quark and -antiquark begin to shed their clothing, gluon emission and subsequent splitting commence [46], and QCD evolution (DGLAP) [47–50] proceeds to generate nonzero glue and sea distributions from the

nonperturbative information contained in $\mathbf{u}^\pi(x; \zeta_{\mathcal{H}})$. Thus, the complex structure in Fig. 1 emerges.

A prediction for the value of $\zeta_{\mathcal{H}}$ follows from the properties of QCD's renormalization group invariant effective charge [10,41,51–54], $\hat{\alpha}(k^2)$. Its scale is set by m_0 , the gluon mass [8,10]. Notwithstanding that, the value of $\zeta_{\mathcal{H}}$ is immaterial herein, so long as Eq. (4) is understood.

Introducing the distribution $\mathcal{P}(t) = \mathbf{u}^\pi([1+t]/2; \zeta_{\mathcal{H}})$, the Mellin moments of the pion valence-quark DF are

$$\langle x^n \rangle_{\mathbf{u}_\pi}^{\zeta_{\mathcal{H}}} = \frac{1}{2^n} \sum_{i=0}^{\lfloor n/2 \rfloor} \binom{n}{2i} \langle t^{2i} \rangle_{\mathcal{P}}, \quad (6)$$

$\langle t^j \rangle_{\mathcal{P}} = \int_0^1 dt t^j \mathcal{P}(t)$. Since the hadron scale DF of a ground-state pseudoscalar meson is necessarily unimodal [8], Sec. 3], two limiting cases are apparent: (i) $\mathcal{P}(t) = \delta(t)$, corresponding to a pion constituted from two infinitely-massive valence constituents; and (ii) its antithesis, $\mathcal{P}(t) = \theta(1+t)\theta(1-t)$, which is obtained for a massless pion using a symmetry-preserving treatment of a vector \times vector contact interaction [55]. They lead to the following bounds:

$$\frac{1}{2^n} \stackrel{(i)}{\leq} \langle x^n \rangle_{\mathbf{u}_\pi}^{\zeta_{\mathcal{H}}} \stackrel{(ii)}{\leq} \frac{1}{1+n}. \quad (7)$$

III. PRINCIPLE AND PRACTICE OF ALL-ORDERS EVOLUTION

We proceed by exploring the consequences of the following hypothesis [42]:

P1—*There exists at least one effective charge, $\alpha_{1\ell}(k^2)$, such that, when used to integrate the one-loop DGLAP equations, an evolution scheme for parton DFs is defined that is all-orders exact.*

Charges of this type are discussed in Refs. [56–58]. They need not be process-independent (PI); hence, not unique. Nevertheless, a suitable PI charge is not excluded, e.g., that discussed in Refs. [10,54] has proved efficacious. In being defined via an observable—in this case, pion structure functions, each such $\alpha_{1\ell}(k^2)$ is [59]: consistent with the renormalization group; renormalization scheme independent; everywhere analytic and finite; and supplies an infrared completion of any standard running coupling.

Regarding this hypothesis, it is worth observing here that CSM results for pion $\zeta = \zeta_{\mathcal{H}}$ valence DFs, obtained from symmetry-preserving analyses and used as initial values for evolution according to **P1**, yield predictions for all pion $\zeta > \zeta_{\mathcal{H}}$ DFs (valence, sea, glue) that are consistent with QCD expectations, including those on their small- and large- x behavior [42,60,61]. Owing to a deficit of pion data [8], Table 9.5], more cannot yet be said. On the other hand, given the large amount of relevant proton data, one might think it possible to test a variant of **P1** using phenomenological proton DF fits [62,63]. Unfortunately,

however, extant such fits are inconsistent with a range of QCD constraints; so, they cannot serve as a reliable foundation for testing the validity of evolution schemes related to **P1**. In large part, this explains conclusions drawn elsewhere [64]. Future such studies should be built upon improved DF fits and use an effective charge that furnishes an infrared completion of QCD.

P1 entails [[65], Sec. VII]

$$\langle x^n \rangle_{\mathbf{u}_\pi}^{\zeta} = \langle x^n \rangle_{\mathbf{u}_\pi}^{\zeta_{\mathcal{H}}} (\langle 2x \rangle_{\mathbf{u}_\pi}^{\zeta})^{\gamma_0^n / \gamma_0^1}, \quad (8)$$

where $\gamma_0^0 = 0$ and, for $n_f = 4$ quark flavors, $\gamma_0^{1,2} = 32/9, 50/9$. The higher- n results are listed elsewhere [[65], Eq. (56a)]. Thus, given the pion valence-quark DF at one scale, e.g., $\zeta_{\mathcal{H}}$, then its pointwise behavior at any other scale, ζ , is fully determined by the value of its first moment at ζ . No other knowledge is required; especially, one need know nothing about the actual form of $\alpha_{1\ell}(k^2)$. Similar statements are true for $\mathbf{g}^\pi(x; \zeta)$, $\mathcal{S}^\pi(x; \zeta)$. As noted above, the hadron scale is uniquely defined by $\langle 2x \rangle_{\mathbf{u}_\pi}^{\zeta_{\mathcal{H}}} = 1$. Inserting Eq. (8) into Eq. (7), one finds:

$$\frac{1}{2^n} \leq \langle x^n \rangle_{\mathbf{u}_\pi}^{\zeta} (\langle 2x \rangle_{\mathbf{u}_\pi}^{\zeta})^{-\gamma_0^n / \gamma_0^1} \leq \frac{1}{1+n}. \quad (9)$$

Together, Eqs. (4), (8) entail this recursion [42]:

$$\begin{aligned} \langle x^{2n+1} \rangle_{\mathbf{u}_\pi}^{\zeta} &= \frac{(\langle 2x \rangle_{\mathbf{u}_\pi}^{\zeta})^{\gamma_0^{2n+1} / \gamma_0^1}}{2(n+1)} \\ &\times \sum_{j=0,1,\dots}^{2n} (-)^j \binom{2(n+1)}{j} \langle x^j \rangle_{\mathbf{u}_\pi}^{\zeta} (\langle 2x \rangle_{\mathbf{u}_\pi}^{\zeta})^{-\gamma_0^j / \gamma_0^1}. \end{aligned} \quad (10)$$

Namely, for any symmetric function, Eq. (4), which evolves according to Eq. (8), the odd-order Mellin moment $\langle x^{2n+1} \rangle_{\mathbf{u}_\pi}^{\zeta}$ is completely determined by the set of even moments $\langle x^{2m} \rangle_{\mathbf{u}_\pi}^{\zeta}$ with $m \leq n$. Conversely, if a DF satisfies Eq. (10), then it is linked by evolution to a symmetric distribution at $\zeta_{\mathcal{H}}$.

IV. PION VALENCE-QUARK DF FROM LATTICE-QCD MOMENTS

Recent years have seen the refinement of lattice-QCD predictions for low-order Mellin moments of the pion valence-quark DF. Some contemporary results are listed in Table I and plotted in Fig. 2. They satisfy the bounds in Eq. (9). Importantly, a calculation which yields points that lie systematically outside the inclusion area does not describe a physically realizable pionlike bound-state; or, stated otherwise, contains systematic uncertainties that preclude its connection with a physical pion-like system.

The moments in Table I—Column 3 [68] satisfy Eq. (10); hence, are associated with a symmetric pion valence-quark

TABLE I. Lattice-QCD results for Mellin moments of the pion valence-quark DF at $\zeta = \zeta_2 = 2$ GeV [66] and $\zeta_5 = 5.2$ GeV [67,68].

n	[66]	[67]	[68]
1	0.254(03)	0.18(3)	0.23(3)(7)
2	0.094(12)	0.064(10)	0.087(05)(08)
3	0.057(04)	0.030(05)	0.041(05)(09)
4			0.023(05)(06)
5			0.014(04)(05)
6			0.009(03)(03)

DF at $\zeta_{\mathcal{H}}$. Here one sees that the moments in Refs. [66,67] are compatible with those in Ref. [68]; so may also be associated with a symmetric DF at $\zeta_{\mathcal{H}}$. Moreover, the consistency between the results in Table I means that one can combine the moments and seek an optimal description of the entire collection.

We therefore consider the symmetric distribution

$$u^\pi(x; \zeta_{\mathcal{H}}) = \mathfrak{n}_0 \ln(1 + x^2(1-x)^2/\rho^2), \quad (11)$$

\mathfrak{n}_0 ensures unit normalization, which is simple yet flexible enough to express the dilation that EHM is known to introduce [10,41,51–54]. Denoting the moments of this distribution by $\mathcal{M}_n^\pi(\rho)$, we minimize the following uncertainty-weighted χ^2 -function:

$$\chi^2(\rho) = \sum_{s=[65-67]} \sum_{n=2}^6 a_n^s \frac{(\mathcal{M}_n^\pi(\rho) - M_n^s(\zeta)/(2M_1^s)^{r_n^s/r_0^s})^2}{(\sigma_n^s)^2}, \quad (12)$$

where $a_n^s = 1$ in all cases with an entry in Table I and is otherwise zero; and $M_n^s(\zeta)$, σ_n^s are the related nonzero

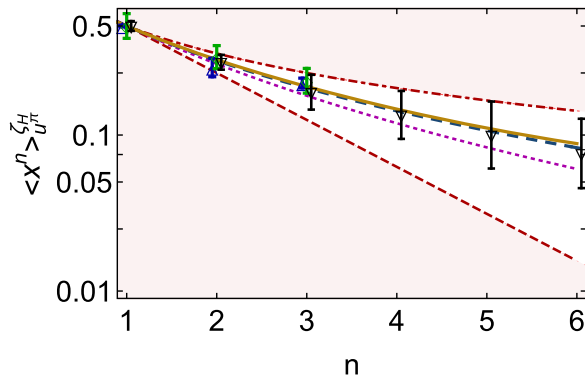


FIG. 2. Mellin moments from Table I, referred to $\zeta_{\mathcal{H}}$ via Eq. (8). Blue up-triangles [66]; green diamonds [67]; and black down-triangles [68]. Results consistent with the bounds in Eq. (9) fall within the open band. The excluded regions are lightly shaded in red. Gold curve: trajectory of moments that minimizes Eq. (12). Long-dashed dark-blue curve: moments of CSM distribution [54]. Dotted magenta curve: moments of the scale-free distribution: $q^{\text{sf}}(x) = 30x^2(1-x)^2$.

entries, *viz.* moment and uncertainty. This yields $\rho_0 = 0.048$ and $\chi^2(\rho_0)/\text{degree-of-freedom} = 0.27$. The associated trajectory of moments is drawn in Fig. 2 (gold curve). It is practically indistinguishable from that calculated using the CSM DF prediction [51–54]. (For subsequent use, we rescale the uncertainties in Eq. (12) such that $\chi_0^2 := \chi^2(\rho_0) = d - 2$, where $d = 8$ is the number of degrees-of-freedom.)

Based on this result, we generate an ensemble of curves that express the uncertainty in the lattice moments as follows. (i) From a distribution centered on ρ_0 , choose a new value of ρ . (ii) Evaluate $\chi^2(\rho)$ in Eq. (12). The new value of ρ is accepted with probability

$$\mathcal{P} = \frac{P(\chi^2; d)}{P(\chi_0^2; d)}, \quad P(y; d) = \frac{(1/2)^{d/2}}{\Gamma(d/2)} y^{d/2-1} e^{-y/2}. \quad (13)$$

(iii) Repeat (i) and (ii) until one has a $K \gtrsim 200$ -member ensemble of DFs. This yields the DFs drawn in Fig. 3(a).

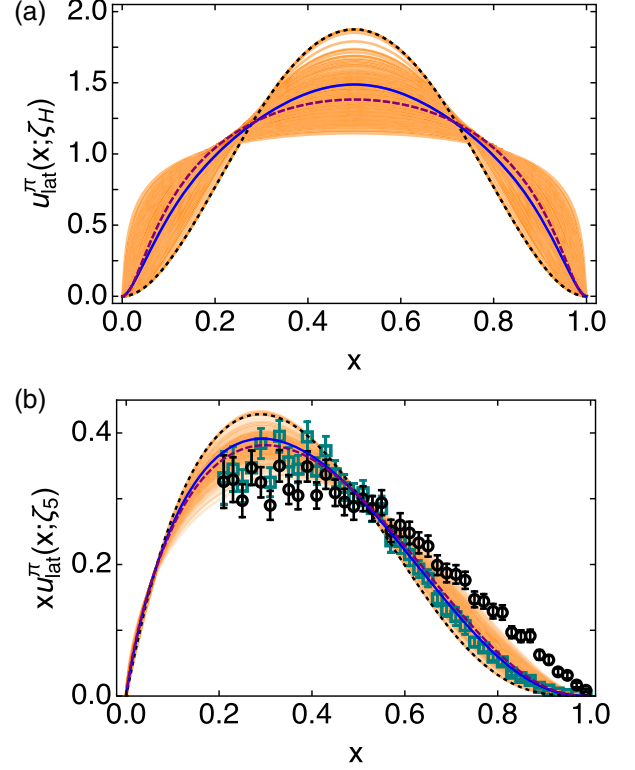


FIG. 3. Upper panel–(a) Randomly distributed ensemble of lattice-QCD-based [66–68] pion valence-quark DFs (orange curves) constructed using the procedure described in connection with Eq. (13). Lower panel–(b) $\zeta_{\mathcal{H}} \rightarrow \zeta_5$ evolution of each curve in Panel (a). Black circles, data recorded in Ref. [40], E615]; and teal boxes, reevaluation of that data as presented in Ref. [69]. Both panels. Dashed magenta curve: central $\rho = \rho_0$ result in Eq. (11). Solid blue curve: CSM prediction from Refs. [41,53,54]. Dotted black curve: scale-free distribution. (All at scale appropriate to panel).

Exploiting P1, every curve in Fig. 3(a) can be evolved to $\zeta_5 = 5.2$ GeV once $\langle 2x \rangle_{u_v}^{\zeta_5}$ is known. Using an uncertainty weighted average of the results in Refs. [54,66–68], which yields $\langle 2x \rangle_{u_v}^{\zeta_5} = 0.435(12)$, and no additional information, one obtains the orange curves in Fig. 3(b). The central curve and associated 1σ -band are reproduced by

$$\mathbf{u}^\pi(x; \zeta_5) = \mathbf{n}_0^{\zeta_5} x^\alpha (1-x)^\beta (1+\gamma x^2), \quad (14)$$

$\alpha = -0.168(79)$, $\beta = 2.49(40)$, $\gamma = 1.51(74)$, with $\mathbf{n}_0^{\zeta_5}$ ensuring unit normalization.

V. PION VALENCE-QUARK DF AT LARGE-X

The results in Fig. 3 bear directly upon a longstanding controversy. Namely [42], analyses of the pion valence-quark DF, which incorporate the behavior of the pion wave function prescribed by QCD, predict

$$\mathbf{u}^\pi(x; \zeta) \approx (1-x)^{\beta=2+\gamma(\zeta)}, \quad (15)$$

where $\gamma(\zeta) \geq 0$ grows logarithmically with ζ , expressing the physics of gluon radiation from the struck quark. As noted above, $\gamma(\zeta_{\mathcal{H}}) = 0$. Nevertheless, more than forty years after the first experiment [37] to deliver data relating to $\mathbf{u}^\pi(x \simeq 1)$, the empirical status remains confused because, among the methods used to fit extant data, *e.g.*, Refs. [69–72], some return a \mathbf{u}^π form that violates Eq. (15). Such disagreement requires that one of the following conclusions be faced: the chosen analysis scheme is incomplete; not all data included are a valid expression of qualities intrinsic to the pion; or QCD, as currently understood, is not the theory of strong interactions.

Fitting the results in Fig. 3(b) on $x \in (0.9, 1)$, one finds the effective value of the large- x exponent: $\beta = 2.45(38)$. Hence, the lattice simulations [66–68] yield a valence-quark DF that is consistent with Eq. (15). However, the leading-order perturbative QCD analysis of data reported in Ref. [40], E615], which disagrees overall with the ensemble of lattice based curves, produces $\beta \approx 1.3$, contradicting Eq. (15). This remains true at next-to-leading-order [70–72]. On the other hand, inclusion of soft-gluon resummation in the hard-scattering kernel produces [69] the teal squares in Fig. 3(b), which agree with the lattice-QCD ensemble and express $\beta = 2.57(6)$, consistent with Eq. (15). The lattice-QCD ensemble also agrees with the CSM prediction [41,53,54], for which $\beta = 2.81(8)$. Recent explorations of uncertainties associated with soft-gluon resummation are briefly discussed in the Appendix.

Given P1, then the results obtained above also enable prediction of the pion glue and sea DFs [[65], Sec. VII]. Using the central curve in Fig. 3(a), obtained with $\rho = \rho_0 = 0.048$ in Eq. (11), one arrives at the DFs in Fig. 4. Within uncertainties, the lattice-QCD based results calculated herein agree with the CSM predictions [41,53,54].

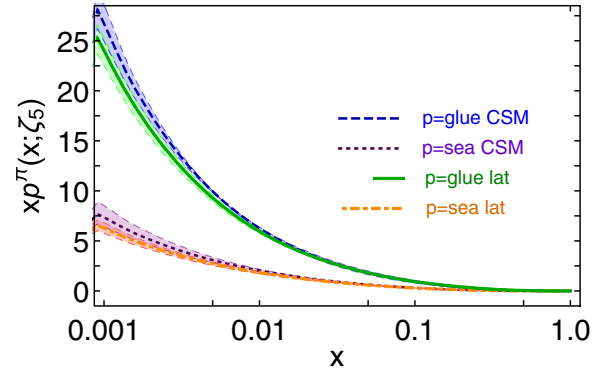


FIG. 4. Glue and sea DFs at $\zeta_5 = 5.2$ GeV. The band associated with each curve expresses consequences of the uncertainty in the valence momentum fraction: $\langle 2x \rangle_{u_v}^{\zeta_5} = 0.435(12)$; leading to $\langle x \rangle_{g_v}^{\zeta_5} = 0.435(06)$, $\langle x \rangle_{S_v}^{\zeta_5} = 0.125(05)$. For comparison, CSM predictions from Refs. [41,53,54] are also drawn: in this case, $\langle 2x \rangle_{u_v}^{\zeta_5} = 0.40(2)$, $\langle x \rangle_{g_v}^{\zeta_5} = 0.45(1)$, $\langle x \rangle_{S_v}^{\zeta_5} = 0.14(1)$.

Notably [41], the CSM result for the glue DF agrees with an independent lattice determination [73]; consequently, so does the result calculated herein.

VI. PERSPECTIVES

More than seventy years after discovery of the pion, Nature’s most fundamental Nambu-Goldstone boson, too little is yet known about its internal structure. This must change if the origin of nuclear-size mass-scales—the emergence of hadron mass—is to be understood within the Standard Model. The proposition considered herein, *viz.* that there is an effective charge which defines an evolution scheme for parton distribution functions (DFs) that is all-orders exact, has many consequences. Among them, the unique definition of the hadron scale, the bounds on all Mellin moments of the valence-quark DF in pionlike systems, and the recursion relation for odd-moments, can be used to good effect, enabling, *e.g.*, parameter-free predictions for all pion DFs that can both benchmark existing data fitting methods and be validated using data from forthcoming experiments. Studies are underway that test the proposition in the nucleon sector [74,75].

ACKNOWLEDGMENTS

We are grateful for constructive comments from O. Denisov, T. Frederico, J. Friedrich, C. Mezrag, V. Mokeev, W.-D. Nowak, J. Papavassiliou, C. Quintans, G. Salmè, and J. Segovia. Work supported by: National Natural Science Foundation of China (Grants No. 12135007, No. 11805097); Helmholtz-Zentrum Dresden-Rossendorf High Potential Programme; Spanish Ministry of Science and Innovation (MICINN) (Grant No. PID2019–107844GB-C22); Junta de Andalucía (Grants No. P18-FR-5057, No. UHU-1264517, No. UHU

EPIT-2021); and STRONG-2020 “The strong interaction at the frontier of knowledge: fundamental research and applications” which received funding from the European Union’s Horizon 2020 research and innovation programme (Grant No. 824093).

APPENDIX: SOFT GLUONS

Uncertainties attendant upon inclusion of soft-gluon resummation in analyses of E615 data are discussed elsewhere [42,72]. Three different methods are compared therein. Two may be described as Mellin-Fourier (MF) schemes [76,77] and yield mutually consistent results. The Ref. [69] analysis is in this class. The third is a double-Mellin (dM) approach [78].

The ensemble of lattice-QCD based results for $u^\pi(x; \zeta_5)$ is compared in Fig. 5 with reanalyses of data using the MF and dM methods. The overall quantitative mismatch between the lattice-QCD based results and both sets of displayed data is explained by the fact that all data fits in Ref. [72] store 15% less of the pion’s longitudinal light-front momentum with the valence degrees-of-freedom than modern calculations predict. Regarding the large- x exponent, the MF approach to soft-gluon resummation (blue

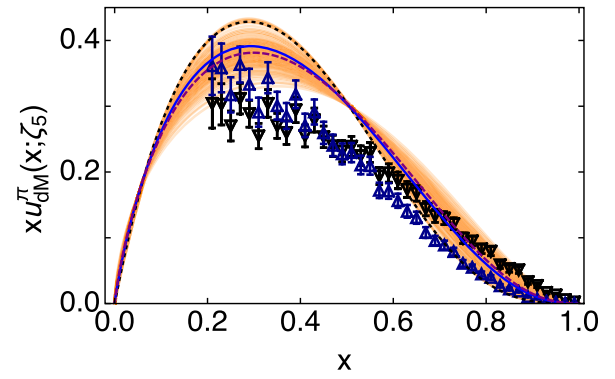


FIG. 5. Orange curves: ensemble of lattice-QCD based results from Fig. 3(b). Black down-triangles, data recorded in Ref. [40], E615] projected onto a double-Mellin fit of pion structure functions; and blue up-triangles, projection onto a Mellin-Fourier fit. (See Ref. [42] for a discussion.) Both panels. Solid blue curve: CSM prediction from Refs. [41,53,54]. Dotted black curve: scale-free distribution.

up-triangles) yields $\beta_{\text{MF}} = 2.24(7)$, agreeing with the lattice result and consistent with Eq. (15). However, the value inferred using the dM scheme, $\beta_{\text{dM}} = 1.54(5)$, is inconsistent with both the lattice result and Eq. (15).

- [1] D. Boyanovsky, H. J. de Vega, and D. J. Schwarz, Phase transitions in the early and the present universe, *Annu. Rev. Nucl. Part. Sci.* **56**, 441 (2006).
- [2] P. Zyla *et al.*, Review of particle physics, *Prog. Theor. Exp. Phys.* **2020**, 083C01 (2020).
- [3] K. D. Lane, Asymptotic freedom and goldstone realization of chiral symmetry, *Phys. Rev. D* **10**, 2605 (1974).
- [4] H. D. Politzer, Effective quark masses in the chiral limit, *Nucl. Phys.* **B117**, 397 (1976).
- [5] W. J. Marciano and H. Pagels, Quantum chromodynamics: A review, *Phys. Rep.* **36**, 137 (1978).
- [6] A. C. Aguilar, D. Binosi, and J. Papavassiliou, Gluon and ghost propagators in the Landau gauge: Deriving lattice results from Schwinger-Dyson equations, *Phys. Rev. D* **78**, 025010 (2008).
- [7] F. Gao, S.-X. Qin, C. D. Roberts, and J. Rodríguez-Quintero, Locating the Gribov horizon, *Phys. Rev. D* **97**, 034010 (2018).
- [8] C. D. Roberts, D. G. Richards, T. Horn, and L. Chang, Insights into the emergence of mass from studies of pion and kaon structure, *Prog. Part. Nucl. Phys.* **120**, 103883 (2021).
- [9] D. Binosi, C. Mezrag, J. Papavassiliou, C. D. Roberts, and J. Rodríguez-Quintero, Process-independent strong running coupling, *Phys. Rev. D* **96**, 054026 (2017).
- [10] Z.-F. Cui, J.-L. Zhang, D. Binosi, F. de Soto, C. Mezrag, J. Papavassiliou, C. D. Roberts, J. Rodríguez-Quintero, J. Segovia, and S. Zafeiropoulos, Effective charge from lattice QCD, *Chin. Phys. C* **44**, 083102 (2020).
- [11] C. D. Roberts, Perspective on the origin of hadron masses, *Few-Body Syst.* **58**, 5 (2017).
- [12] C. D. Roberts, A. G. Williams, and G. Krein, On the implications of confinement, *Int. J. Mod. Phys. A* **07**, 5607 (1992).
- [13] D. Binosi and R.-A. Tripolt, Spectral functions of confined particles, *Phys. Lett. B* **801**, 135171 (2020).
- [14] G. Eichmann, H. Sanchis-Alepuz, R. Williams, R. Alkofer, and C. S. Fischer, Baryons as relativistic three-quark bound states, *Prog. Part. Nucl. Phys.* **91**, 1 (2016).
- [15] C. S. Fischer, QCD at finite temperature and chemical potential from Dyson–Schwinger equations, *Prog. Part. Nucl. Phys.* **105**, 1 (2019).
- [16] S.-X. Qin and C. D. Roberts, Impressions of the continuum bound state problem in QCD, *Chin. Phys. Lett.* **37**, 121201 (2020).
- [17] C. D. Roberts, Empirical consequences of emergent mass, *Symmetry* **12**, 1468 (2020).
- [18] T. Horn and C. D. Roberts, The pion: An enigma within the Standard Model, *J. Phys. G* **43**, 073001 (2016).
- [19] P. Maris and C. D. Roberts, π and K meson Bethe-Salpeter amplitudes, *Phys. Rev. C* **56**, 3369 (1997).
- [20] A. Höll, A. Krassnigg, and C. D. Roberts, Pseudoscalar meson radial excitations, *Phys. Rev. C* **70**, 042203 (2004).
- [21] S.-X. Qin, C. D. Roberts, and S. M. Schmidt, Ward-Green-Takahashi identities and the axial-vector vertex, *Phys. Lett. B* **733**, 202 (2014).

- [22] R. Williams, C. S. Fischer, and W. Heupel, Light mesons in QCD and unquenching effects from the 3PI effective action, *Phys. Rev. D* **93**, 034026 (2016).
- [23] D. Binosi, L. Chang, S.-X. Qin, J. Papavassiliou, and C. D. Roberts, Symmetry preserving truncations of the gap and Bethe-Salpeter equations, *Phys. Rev. D* **93**, 096010 (2016).
- [24] S.-X. Qin and C. D. Roberts, Resolving the Bethe-Salpeter kernel, *Chin. Phys. Lett.* **38**, 071201 (2021).
- [25] D. Carman, K. Joo, and V. Mokeev, Strong QCD insights from excited nucleon structure studies with CLAS and CLAS12, *Few-Body Syst.* **61**, 29 (2020).
- [26] S. J. Brodsky *et al.*, Strong QCD from hadron structure experiments, *Int. J. Mod. Phys. E* **29**, 2030006 (2020).
- [27] M. Y. Barabanov *et al.*, Diquark correlations in hadron physics: Origin, impact and evidence, *Prog. Part. Nucl. Phys.* **116**, 103835 (2021).
- [28] C. Keppel, B. Wojtsekhowski, P. King, D. Dutta, J. Annand, J. Zhang *et al.*, Measurement of tagged deep inelastic scattering (TDIS) approved Jefferson Lab experiment, Report No. E12-15-006.
- [29] K. Park, R. Montgomery, T. Horn *et al.*, Measurement of kaon structure function through tagged deep inelastic scattering (TDIS) approved Jefferson Lab experiment, Report No. C12-15-006A.
- [30] B. Adams *et al.*, Letter of intent: A new QCD facility at the M2 beam line of the CERN SPS (COMPASS+/AMBER), arXiv:1808.00848.
- [31] A. C. Aguilar *et al.*, Pion and kaon structure at the electron-ion collider, *Eur. Phys. J. A* **55**, 190 (2019).
- [32] X. Chen, F.-K. Guo, C. D. Roberts, and R. Wang, Selected science opportunities for the EicC, *Few-Body Syst.* **61**, 43 (2020).
- [33] D. P. Anderle *et al.*, Electron-ion collider in China, *Front. Phys. (Beijing)* **16**, 64701 (2021).
- [34] J. Arrington *et al.*, Revealing the structure of light pseudoscalar mesons at the electron-ion collider, *J. Phys. G* **48**, 075106 (2021).
- [35] R. J. Holt and C. D. Roberts, Distribution functions of the nucleon and pion in the valence region, *Rev. Mod. Phys.* **82**, 2991 (2010).
- [36] C. D. Roberts and A. G. Williams, Dyson-Schwinger equations and their application to hadronic physics, *Prog. Part. Nucl. Phys.* **33**, 477 (1994).
- [37] M. Corden *et al.*, Production of muon pairs in the continuum region by 39.5-GeV/c π^\pm , K^\pm , p and \bar{p} beams incident on a tungsten target, *Phys. Lett. B* **96**, 417 (1980).
- [38] J. Badier *et al.*, Experimental determination of the π -meson structure functions by the Drell-Yan mechanism, *Z. Phys. C* **18**, 281 (1983).
- [39] B. Betev *et al.*, Observation of anomalous scaling violation in muon pair production by 194-GeV/c π -tungsten interactions, *Z. Phys. C* **28**, 15 (1985).
- [40] J. S. Conway *et al.*, Experimental study of muon pairs produced by 252-GeV pions on tungsten, *Phys. Rev. D* **39**, 92 (1989).
- [41] L. Chang and C. D. Roberts, Regarding the distribution of glue in the pion, *Chin. Phys. Lett.* **38**, 081101 (2021).
- [42] Z. F. Cui, M. Ding, J. M. Morgado, K. Raya, D. Binosi, L. Chang, J. Papavassiliou, C. D. Roberts, J. Rodríguez-Quintero, and S. M. Schmidt, Concerning pion parton distributions, *Eur. Phys. J. A* **58**, 10 (2022).
- [43] G. 't Hooft, A two-dimensional model for mesons, *Nucl. Phys.* **B75**, 461 (1974).
- [44] L. Chang, I. C. Cloet, J. J. Cobos-Martinez, C. D. Roberts, S. M. Schmidt, and P. C. Tandy, Imaging Dynamical Chiral Symmetry Breaking: Pion Wave Function on the Light Front, *Phys. Rev. Lett.* **110**, 132001 (2013).
- [45] M. Diehl, T. Feldmann, R. Jakob, and P. Kroll, The overlap representation of skewed quark and gluon distributions, *Nucl. Phys.* **B596**, 33 (2001).
- [46] S. J. Brodsky and G. P. Lepage, Perturbative quantum chromodynamics, *Prog. Math. Phys.* **4**, 255 (1979).
- [47] Y. L. Dokshitzer, Calculation of the structure functions for deep inelastic scattering and $e + e^-$ annihilation by perturbation theory in quantum chromodynamics. (In Russian), *Sov. Phys. JETP* **46**, 641 (1977).
- [48] V. N. Gribov and L. N. Lipatov, Deep inelastic electron scattering in perturbation theory, *Phys. Lett. B* **37**, 78 (1971).
- [49] L. N. Lipatov, The parton model and perturbation theory, *Sov. J. Nucl. Phys.* **20**, 94 (1975).
- [50] G. Altarelli and G. Parisi, Asymptotic freedom in parton language, *Nucl. Phys.* **B126**, 298 (1977).
- [51] M. Ding, K. Raya, D. Binosi, L. Chang, C. D. Roberts, and S. M. Schmidt, Drawing insights from pion parton distributions, *Chin. Phys. C* **44**, 031002 (2020).
- [52] M. Ding, K. Raya, D. Binosi, L. Chang, C. D. Roberts, and S. M. Schmidt, Symmetry, symmetry breaking, and pion parton distributions, *Phys. Rev. D* **101**, 054014 (2020).
- [53] Z.-F. Cui, M. Ding, F. Gao, K. Raya, D. Binosi, L. Chang, C. D. Roberts, J. Rodríguez-Quintero, and S. M. Schmidt, Higgs modulation of emergent mass as revealed in kaon and pion parton distributions, *Eur. Phys. J. A* **57**, 5 (2021).
- [54] Z.-F. Cui, M. Ding, F. Gao, K. Raya, D. Binosi, L. Chang, C. D. Roberts, J. Rodríguez-Quintero, and S. M. Schmidt, Kaon and pion parton distributions, *Eur. Phys. J. C* **80**, 1064 (2020).
- [55] J.-L. Zhang, Z.-F. Cui, J. Ping, and C. D. Roberts, Contact interaction analysis of pion GTMDs, *Eur. Phys. J. C* **81**, 6 (2021).
- [56] G. Grunberg, Renormalization scheme independent QCD and QED: The method of effective charges, *Phys. Rev. D* **29**, 2315 (1984).
- [57] G. Grunberg, On some ambiguities in the method of effective charges, *Phys. Rev. D* **40**, 680 (1989).
- [58] Y. L. Dokshitzer, Perturbative QCD theory (includes our knowledge of $\alpha(s)$), in *Proceedings of the 29th International Conference on High-Energy Physics, ICHEP'98, Vancouver, Canada, 1998* (1998), Vol. 1, 2, pp. 305–324, arXiv:hep-ph/9812252.
- [59] A. Deur, S. J. Brodsky, and G. F. de Teramond, The QCD running coupling, *Prog. Part. Nucl. Phys.* **90**, 1 (2016).
- [60] S. J. Brodsky, M. Burkardt, and I. Schmidt, Perturbative QCD constraints on the shape of polarized quark and gluon distributions, *Nucl. Phys.* **B441**, 197 (1995).
- [61] F. Yuan, Generalized parton distributions at $x \rightarrow 1$, *Phys. Rev. D* **69**, 051501 (2004).
- [62] R. D. Ball *et al.*, Parton distributions from high-precision collider data, *Eur. Phys. J. C* **77**, 663 (2017).

- [63] T.-J. Hou *et al.*, New CTEQ global analysis of quantum chromodynamics with high-precision data from the LHC, *Phys. Rev. D* **103**, 014013 (2021).
- [64] M. Diehl and P. Stienemeier, Gluons and sea quarks in the proton at low scales, *Eur. Phys. J. Plus* **135**, 211 (2020).
- [65] K. Raya, Z.-F. Cui, L. Chang, J.-M. Morgado, C. D. Roberts, and J. Rodríguez-Quintero, Revealing pion and kaon structure via generalised parton distributions, *Chin. Phys. C* **46**, 013105 (2022).
- [66] B. Joó, J. Karpie, K. Orginos, A. V. Radyushkin, D. G. Richards, R. S. Sufian, and S. Zafeiropoulos, Pion valence structure from Ioffe-time parton pseudodistribution functions, *Phys. Rev. D* **100**, 114512 (2019).
- [67] R. S. Sufian, J. Karpie, C. Egerer, K. Orginos, J.-W. Qiu, and D. G. Richards, Pion valence quark distribution from matrix element calculated in lattice QCD, *Phys. Rev. D* **99**, 074507 (2019).
- [68] C. Alexandrou, S. Bacchio, I. Cloet, M. Constantinou, K. Hadjiyiannakou, G. Koutsou, and C. Lauer, Pion and kaon $\langle x^3 \rangle$ from lattice QCD and PDF reconstruction from Mellin moments, *Phys. Rev. D* **104**, 054504 (2021).
- [69] M. Aicher, A. Schäfer, and W. Vogelsang, Soft-Gluon Resummation and the Valence Parton Distribution Function of the Pion, *Phys. Rev. Lett.* **105**, 252003 (2010).
- [70] I. Novikov *et al.*, Parton distribution functions of the charged pion within The xFitter framework, *Phys. Rev. D* **102**, 014040 (2020).
- [71] C. Han, G. Xie, R. Wang, and X. Chen, An analysis of parton distribution functions of the pion and the kaon with the maximum entropy input, *Eur. Phys. J. C* **81**, 302 (2021).
- [72] P. C. Barry, C.-R. Ji, N. Sato, and W. Melnitchouk, Global QCD Analysis of Pion Parton Distributions with Threshold Resummation, *Phys. Rev. Lett.* **127**, 232001 (2021).
- [73] Z. Fan and H.-W. Lin, Gluon parton distribution of the pion from lattice QCD, *Phys. Lett. B* **823**, 136778 (2021).
- [74] L. Chang, F. Gao, and C. D. Roberts, Parton distributions of light quarks and antiquarks in the proton, *Phys. Lett. B* **829**, 137078 (2022).
- [75] Y. Lu, L. Chang, K. Raya, C. D. Roberts, and J. Rodríguez-Quintero, Proton and pion distribution functions in counterpoint, *Phys. Lett. B* **830**, 137130 (2022).
- [76] G. F. Sterman and W. Vogelsang, Threshold resummation and rapidity dependence, *J. High Energy Phys.* **02** (2001) 016.
- [77] A. Mukherjee and W. Vogelsang, Threshold resummation for W-boson production at RHIC, *Phys. Rev. D* **73**, 074005 (2006).
- [78] D. Westmark and J. F. Owens, Enhanced threshold resummation formalism for lepton pair production and its effects in the determination of parton distribution functions, *Phys. Rev. D* **95**, 056024 (2017).